

## ***Paired windward and leeward biogeochemical time series reveal consistent surface ocean CO<sub>2</sub> trends across the Hawaiian Ridge***

The Faculty of Oregon State University has made this article openly available.  
Please share how this access benefits you. Your story matters.

<b>Citation</b>	Dore, J. E., Church, M. J., Karl, D. M., Sadler, D. W., & Letelier, R. M. (2014). Paired windward and leeward biogeochemical time series reveal consistent surface ocean CO <sub>2</sub> trends across the Hawaiian Ridge. <i>Geophysical Research Letters</i> , 41(18), 6459-6467. doi:10.1002/2014GL060725
<b>DOI</b>	10.1002/2014GL060725
<b>Publisher</b>	American Geophysical Union
<b>Version</b>	Version of Record
<b>Terms of Use</b>	<a href="http://cdss.library.oregonstate.edu/sa-termsfuse">http://cdss.library.oregonstate.edu/sa-termsfuse</a>



## RESEARCH LETTER

10.1002/2014GL060725

## Key Points:

- Annual cycles and secular trends explain much surface CO<sub>2</sub> temporal variability
- Physically contrasting time-series sites yield common biogeochemical trends
- Ocean acidification rates on either side of the Hawaiian Ridge are identical

## Supporting Information:

- Readme
- Figure S1
- Figure S2
- Table S1

## Correspondence to:

J. E. Dore,  
jdore@montana.edu

## Citation:

Dore, J. E., M. J. Church, D. M. Karl, D. W. Sadler, and R. M. Letelier (2014), Paired windward and leeward biogeochemical time series reveal consistent surface ocean CO<sub>2</sub> trends across the Hawaiian Ridge, *Geophys. Res. Lett.*, *41*, 6459–6467, doi:10.1002/2014GL060725.

Received 30 MAY 2014

Accepted 1 SEP 2014

Accepted article online 3 SEP 2014

Published online 22 SEP 2014

## Paired windward and leeward biogeochemical time series reveal consistent surface ocean CO<sub>2</sub> trends across the Hawaiian Ridge

John E. Dore<sup>1</sup>, Matthew J. Church<sup>2</sup>, David M. Karl<sup>2</sup>, Daniel W. Sadler<sup>2</sup>, and Ricardo M. Letelier<sup>3</sup>

<sup>1</sup>Department of Land Resources and Environmental Sciences, Montana State University, Bozeman, Montana, USA,

<sup>2</sup>Department of Oceanography, University of Hawai'i at Mānoa, Honolulu, Hawaii, USA, <sup>3</sup>College of Earth, Ocean, and Atmospheric Sciences, Oregon State University, Corvallis, Oregon, USA

**Abstract** Sustained time series have provided compelling evidence for progressive acidification of the surface oceans through exchange with the growing atmospheric reservoir of carbon dioxide. However, few long-term programs exist, and extrapolation of results from one site to larger oceanic expanses is hampered by the lack of spatial coverage inherent to Eulerian sampling. Since 1988, the Hawaii Ocean Time-series program has sampled CO<sub>2</sub> system variables nearly monthly at Station ALOHA, a deep ocean site windward and 115 km north of the island of Oahu. Surface measurements have also been made at Station Kahe, a leeward site 12 km from the island and on the opposite side of the Hawaiian Ridge. Despite having different physical settings, the sites exhibit identical rates of surface pCO<sub>2</sub> increase and hydrogen ion accumulation, suggesting that atmospheric forcing dominates over local dynamics in determining the CO<sub>2</sub> trend in the surface waters of the North Pacific subtropical gyre.

### 1. Introduction

Oceans are key regulators of planetary climate and global biogeochemical cycles. Among their many functions is the exchange of carbon dioxide (CO<sub>2</sub>) with the atmosphere. The magnitude and direction of this exchange are spatially and temporally variable and are governed by both physical and biological factors; nevertheless, there is evidence of an open ocean secular increase of dissolved inorganic carbon (DIC) in response to the rapidly rising anthropogenic CO<sub>2</sub> in the atmosphere [Dore *et al.*, 2009; Bates *et al.*, 2014]. The resulting acidification of surface waters could have profound impacts on ocean ecosystem structure and function [Doney *et al.*, 2009; Kroeker *et al.*, 2013]. Ocean biogeochemical time series are among our most important tools for assessing such changes and for placing spatial survey data into a temporal context; yet only a handful of such programs exists [Church *et al.*, 2013], and results from these benchmark sites are commonly extrapolated to larger geographic scales. However, seldom are parallel time series data sets within a single region available for direct comparison, with the notable exceptions of those from the Bermuda Atlantic Time-series Study and Hydrostation S sites near Bermuda [Gruber *et al.*, 2002; Phillips and Joyce, 2007] and those from Stations ALOHA (A Long-term Oligotrophic Habitat Assessment) and Kahe near Hawaii (Figure S1 in the supporting information), which we discuss here.

Station ALOHA (22.75°N, 158°W) is a deep ocean (~4750 m) site windward and 115 km north of the island of Oahu and serves as the primary research site for the Hawaii Ocean Time-series (HOT) program. The location chosen for ALOHA was a trade-off between sufficient distance from land, transit time, and other logistics [Karl and Lukas, 1996]. ALOHA was intended to be representative of the open ocean in the North Pacific subtropical gyre (NPSG). However, rigorous criteria were not available for guiding the distance from land chosen, with the one exception being the stratification- and latitude-dependent Rossby radius of deformation (in this case 45 km). Since ALOHA was established, we have come to understand that the inherent spatial variability in the NPSG is greater than believed, complicating the development of criteria for “sufficient distance” to avoid terrestrial effects.

The Hawaiian Ridge serves as a formidable yet semiporous barrier to the Northeast Trade Winds [Xie *et al.*, 2001] and the North Equatorial Current [Roden, 1991; Chavanne *et al.*, 2010]; complex mesoscale and submesoscale ocean circulation features result from their interactions. Mean flow on both sides of the ridge

is west-northwestward in the form of the Hawaiian Ridge Current and the Hawaiian Lee Current, which flow along the windward and leeward coasts, respectively [Lumpkin and Flament, 2013]. However, flow along the ridge is dominated by an energetic mesoscale eddy field [Qiu *et al.*, 1997], and eddy kinetic energy is particularly strong in the immediate lee of the islands, where wake instability leads to the formation of vigorous cyclonic and anticyclonic vortices [Chavanne *et al.*, 2010]. Due to differences in winds, currents, and eddy fields, one might expect to find differences in the temporal dynamics of biogeochemical variables across the barrier, including those of the CO<sub>2</sub>-carbonic acid system [e.g., Chen *et al.*, 2008]. Moreover, the existence of a Hawaiian “island mass effect,” enriching nearshore relative to open ocean plankton biomass, has been debated for decades [Doty and Oguri, 1956; Gilmartin and Revelante, 1974; Hassett and Boehlert, 1999]. Some coastal locations in other regions have yielded ocean acidification rates considerably greater than those expected from atmospheric CO<sub>2</sub> equilibration, with underlying causes that are still unclear [Provoost *et al.*, 2010; Wootton and Pfister, 2012]. Nevertheless, existing information on changes in ocean biogeochemistry encountered across the windward/leeward transition or with proximity to the island masses in the Hawaiian region is limited in temporal scope and resolution.

Here we present a comparison of the 24 year surface ocean biogeochemical time series of ALOHA with the record from Station Kahe (21.343°N, 158.273°W), a leeward site 12 km from Oahu. Since October 1988, intensive ship-based physical and biogeochemical sampling at ALOHA has been carried out at an average occupation frequency of 10 cruises year<sup>-1</sup>. Kahe, while used primarily for testing seagoing equipment, is also regularly sampled for a limited subset of variables. Despite its relative proximity to shore, Kahe has a depth of ~1550 m (owing to steep island topography), and thus, it is well beyond the 200 m isobath commonly used to define “coastal” ecosystems. The site is also off a relatively dry coastline, which limits riverine inputs to the sea. Thus, Kahe may be considered a “replicate” time series to ALOHA, albeit one with a complicated physical oceanographic setting and a greater potential for terrestrial influence.

## 2. Methods

Temperature and salinity measurements and discrete water samples were collected using a conductivity-temperature-depth rosette system following standard HOT program procedures [Karl and Lukas, 1996; Lukas and Santiago-Mandujano, 1996]. Mixed layer depth (MLD) was determined based on a potential density change of 0.125 kg m<sup>-3</sup> from the surface value; this value prevents the diurnal shoaling of the actively mixing layer from aliasing MLD estimates. Chlorophyll *a* (chl *a*) was determined by fluorometry [Letelier *et al.*, 1996]. DIC was measured by coulometry and total alkalinity (TA) by acid titration; certified seawater CO<sub>2</sub> reference materials were used to validate DIC and TA calibrations [Dickson *et al.*, 2007]. Salinity normalization of these parameters was used to calculate *n*DIC (= 35 × DIC/salinity) and *n*TA (= 35 × TA/salinity). Seawater CO<sub>2</sub> partial pressure (*p*CO<sub>2</sub>), hydrogen ion concentration ([H<sup>+</sup>] = 10<sup>-pH</sup>, where pH is measured on the total scale), and aragonite saturation state (Ω<sub>arag</sub>) were calculated from DIC and TA using the CO2SYS software [Pierrot *et al.*, 2006] to solve the equilibrium equations for the dissolved carbonic acid system, as described in Dore *et al.* [2009]. Validation of [H<sup>+</sup>] results and the internal consistency of CO<sub>2</sub> system calculations was achieved through comparison of calculated values with direct colorimetric pH measurements [Clayton and Byrne, 1993; Dore *et al.*, 2009]. Sea surface atmospheric CO<sub>2</sub> partial pressure (*p*CO<sub>2atm</sub>) was derived from monthly mean dry air mole fractions measured at the Mauna Loa Observatory [Keeling *et al.*, 2009; Thoning *et al.*, 2014], using monthly mean sea surface temperatures and barometric pressures from ALOHA and an assumed 85% relative humidity.

We consider here only values from the surface ocean for all parameters except MLD and *p*CO<sub>2atm</sub>. We define the surface layer at ALOHA as the upper 30 m [Dore *et al.*, 2009], while at Kahe we consider only the upper 20 m, in order to minimize the potential impact of samples from below the mixed layer, which is usually shallower at Kahe than at ALOHA. In most cases, the values from ALOHA represent occupation means from samples collected near 5 and 25 m, while at Kahe the values are typically from single samples collected at 5 m. In order to facilitate spectral analyses, the irregularly spaced time series of the variables considered at each site were converted by linear interpolation to vectors sharing a common temporal spacing of 0.1 year. For all variables at ALOHA, 240-point vectors, beginning in November 1988 and ending in October 2012, were constructed. Parallel interpolated vectors were prepared from Kahe data, except, due to missing early data, vectors for ocean CO<sub>2</sub> variables and chl *a* could only be constructed beginning in March 1991 (217 points) and November 1989 (230 points), respectively.

In order to identify significant periodicities in the interpolated data vectors, we employed the nonparametric Multitaper Method (MTM) of spectral analysis with a robust estimation of background signal noise [Thomson, 1982; Mann and Lees, 1996; Ghil et al., 2002]. This approach allows for significance testing of both truly harmonic and quasiperiodic narrowband signals against a red noise background, which is characteristic of time-dependent climatic and geophysical phenomena [Mann and Lees, 1996; Deser et al., 2003]. Other advantages of MTM are that no a priori model need be assumed to underlie the analyzed time series and that both amplitude and phase modulation of sinusoids used for signal reconstruction are allowed [Ghil et al., 2002]. Moreover, the robust noise estimation allows for spectral analysis to be carried out without prior removal of secular trends [Mann and Lees, 1996]. The analysis was carried out using the kSpectra 3.4.1 software toolkit (SpectraWorks), using three tapers, default resolution and normalization settings, and an adaptive spectrum estimation procedure. Long-term secular trends could not be resolved from signals with  $>12$ ,  $>10.85$ , or  $>11.5$  year periods for the 24.0, 21.7, and 23.0 year data vectors, respectively [Mann and Lees, 1996]; hence, deviations from linearity in the secular signals should be interpreted with caution, as they may or may not indicate the existence of true decadal or lower frequency signals. Narrowband signals with approximately annual and shorter periods that were determined to be significantly ( $>95\%$  confidence) above background red noise were then isolated and subtracted from the data vectors in order to “deseasonalize” each time series. Mean values of the deseasonalized data were compared between sites with a two-tailed  $t$  test. Where secular trends had been detected ( $>90\%$  confidence) by the MTM analysis, ordinary linear regressions were performed on the deseasonalized vectors to estimate long-term linear rates of change. Further subtraction of mean values or (where applicable) these linear trends then yielded residuals, which were compared between sites by difference and by cross correlation.

### 3. Results

Selected variables from ALOHA and Kahe display multiple time scales of variability including a prominent annual cycle (Figure 1). The MTM frequency spectra of the data vectors from the two sites (analyzed over the longest directly comparable time windows) exhibit similar patterns for any given variable, but there are some important distinctions in the timescales of periodicity observed for different variables (Figure 2 and Table S1). The annual signal near  $1 \text{ year}^{-1}$  is highly significant ( $>99\%$  confidence) for all variables except  $nTA$ . The  $\text{CO}_2$  system variables  $p\text{CO}_2$ ,  $[\text{H}^+]$ , and  $n\text{DIC}$  also display significant ( $>95\%$  confidence) secular trends at both sites, as does  $nTA$  at ALOHA (Table 1). Salinity and  $\Omega_{\text{arag}}$  at both sites and  $nTA$  at Kahe also display trends, though of lower confidence ( $>90\%$ ). No significant trends in temperature, MLD, or chl  $a$  were detected by the MTM analysis at either site. Also, no narrowband signals with periods between  $\sim 1$  year and a decade were detected in any data set. High-frequency signals (periods  $< \sim 1$  year) were detected in nearly all data sets, with varying levels of significance.

After removing significant annual and high-frequency signals from the data vectors (see section 2), linear regressions were performed where secular trends had been detected with  $>90\%$  confidence (Table 1). All the rates of change so derived are statistically indistinguishable between ALOHA and Kahe (based on  $95\%$  confidence intervals of regression slopes). Mean deseasonalized values reveal that Kahe surface waters are warmer and fresher than those at ALOHA (Table 2). In addition, Kahe has shallower mixed layers and lower chl  $a$  than does ALOHA. Small ( $<2\%$ ) but significant ( $p < 0.05$ ) differences between ALOHA and Kahe means were noted for all ocean  $\text{CO}_2$  system variables (Table 2). Residuals remaining after removal of means or (where applicable) linear trends from the deseasonalized data are generally small, with some exceptions (Table 2 and Figure S2). The root-mean-square (RMS) of residuals was  $\leq 2.5\%$  of the overall mean value for all variables except chl  $a$  and MLD, which exhibited RMS values from 22.3 to 26.4% and 27.0 to 38.4% of their corresponding means, respectively. The strongest correlations of residual signals between ALOHA and Kahe were in all cases obtained without any time lag, and the observed unlagged correlations varied widely in strength between variables tested (Table 2). Residuals were the largest contributor to variance at both sites for  $nTA$ , salinity, chl  $a$ , and MLD, while annual and higher-frequency narrowband signals and/or linear trends dominated the variance of the other variables tested (Table 3).

### 4. Discussion and Conclusions

MTM spectral analysis of the ALOHA and Kahe data sets reveals that annual periodicity and (where present) long-term secular trends contribute strongly to observed temporal variability in surface ocean physical

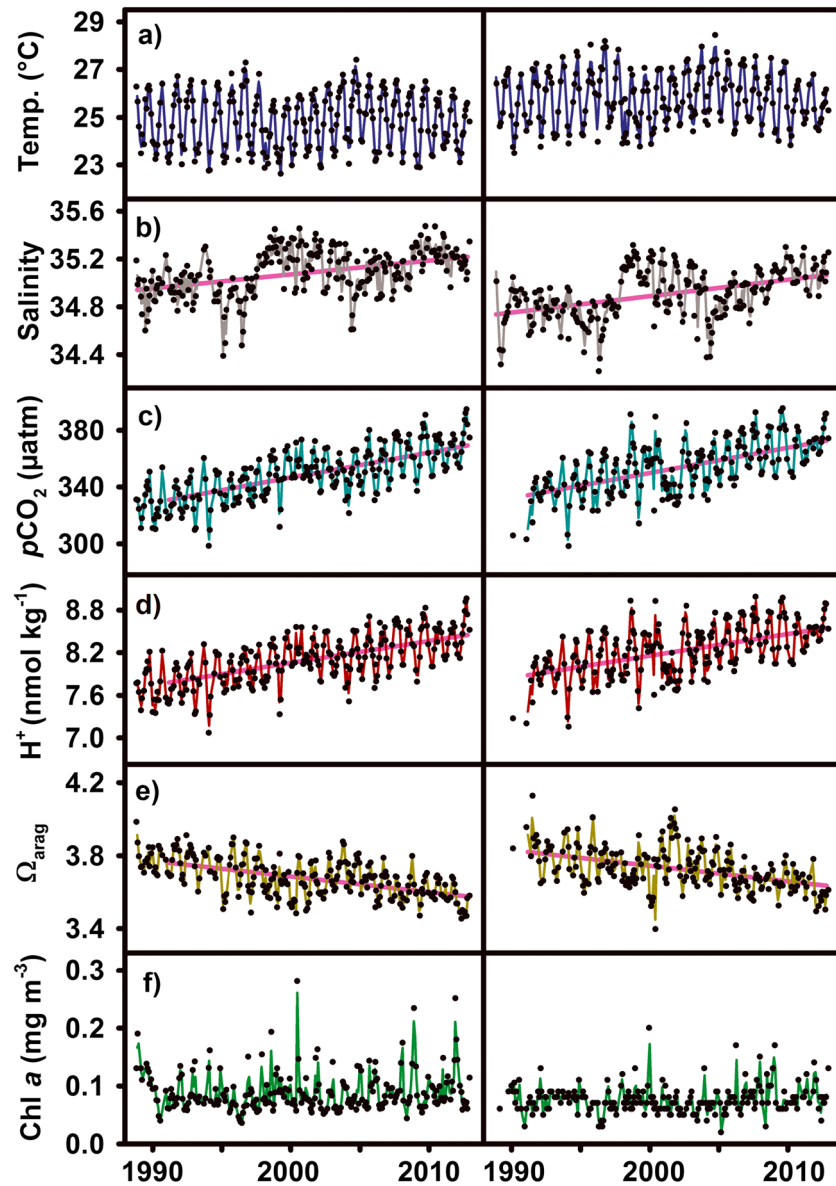


**Figure 1.** Time series of selected surface ocean physical and biogeochemical variables at (left column) Stations ALOHA and (right column) Kahe, 1988–2012. Parameters displayed are the following: (a) temperature, (b) salinity, (c) partial pressure of CO<sub>2</sub>, (d) hydrogen ion concentration, (e) aragonite saturation state, and (f) chlorophyll *a* concentration. Raw data (symbols) were linearly interpolated to produce data vectors (solid curves) with 0.1 year spacing. Magenta lines represent linear temporal trends of data vectors following deseasonalization, where significant (>90% confidence) trends were detected by Multitaper spectral analysis (see section 2). The trends shown are those calculated for the time periods where Kahe data are complete, to facilitate direct comparison between stations.

and biogeochemical variables in the NPSG. The annual cycle of CO<sub>2</sub> system variables is similar between sites (Figure 1) and is likely driven by similar processes. At ALOHA, winter mixing entrains DIC, while the temperature-dependent uptake of atmospheric CO<sub>2</sub> occurs mainly in spring and removal of DIC by net biological production peaks in summer [Dore *et al.*, 2003; Keeling *et al.*, 2004]; advection may also contribute to the DIC budget, but the magnitude of this term is a matter of debate and its potential seasonality is unclear [Keeling *et al.*, 2004; Dore *et al.*, 2009]. Higher-frequency variability (>1 year<sup>-1</sup>) at both sites is also observed in these data sets and could derive from a number of sources. Signals centered near 2 year<sup>-1</sup> and 3 year<sup>-1</sup> (e.g., for temperature and pCO<sub>2</sub>) may represent harmonics of the annual cycle, while some

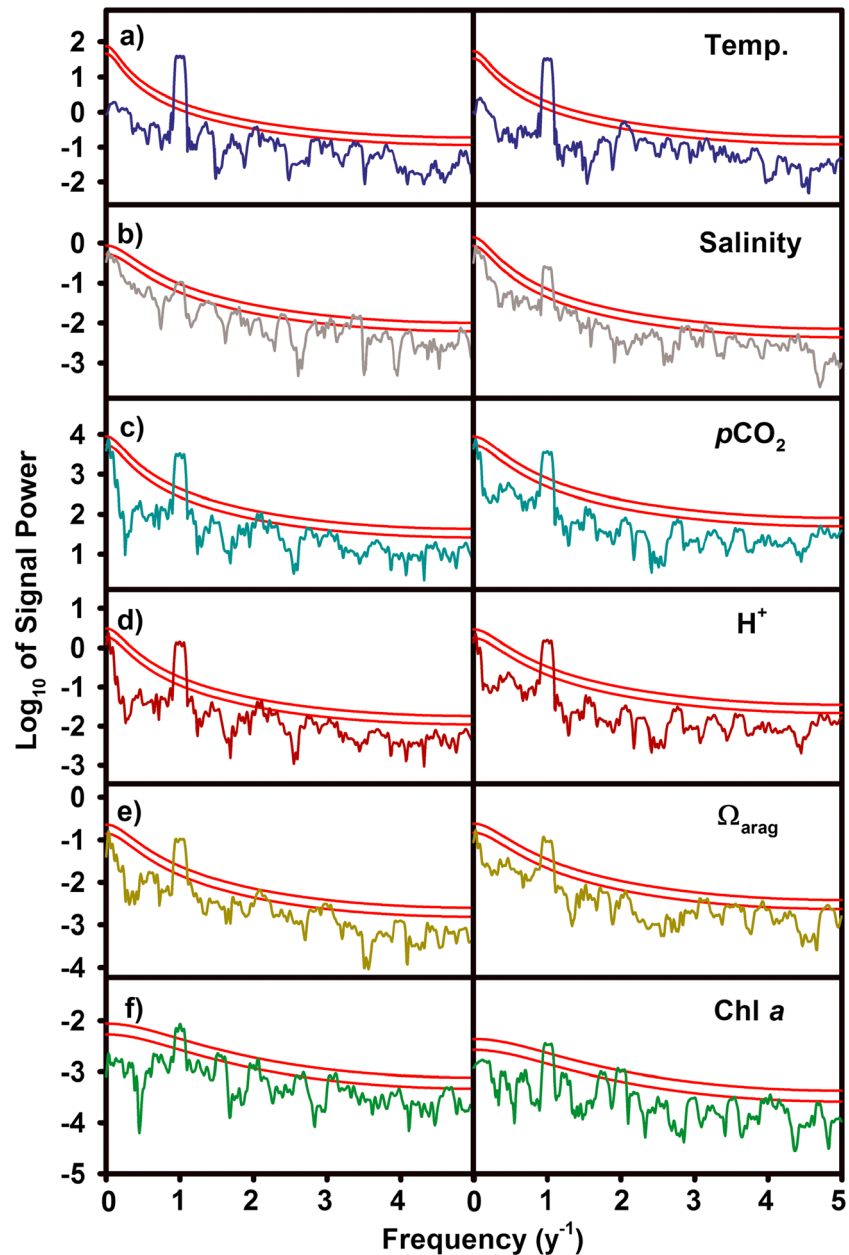


**Figure 2.** Results of Multitaper spectral analyses of the interpolated data vectors from Figure 1. Each panel shows the common logarithm of signal power (solid curves) as a function of signal frequency ( $\text{year}^{-1}$ ). Red curves indicate 90% (lower) and 99% (upper) confidence levels that the observed signals exceed a robust red noise background. The power spectra shown are calculated for the time periods where Kahe data are complete, to facilitate direct comparison between stations: (a, b) November 1988 to October 2012, (c–e) March 1991 to October 2012, (f) November 1989 to October 2012.

signals between 1.5 and 4.5  $\text{year}^{-1}$  (e.g., for  $n\text{DIC}$  and  $\text{chl } a$ ) could be related to the physical impact of mesoscale eddies [Letelier *et al.*, 2000] or Rossby waves [Sakamoto *et al.*, 2004] on nutricline dynamics. However, signals with frequencies approaching 5  $\text{year}^{-1}$  should be interpreted with caution and may simply represent aliasing noise, as this frequency is the Nyquist frequency for the data sets. Regardless, all significant ( $>95\%$  confidence) high-frequency signals were small compared to annual signals. Although quasiperiodic (3–8 years) El Niño–Southern Oscillation (ENSO) related impacts on the ALOHA ecosystem have previously been suggested [Karl *et al.*, 1995], significant low-frequency signals (periods  $> \sim 1$  but  $< \sim 10$  years) were not detected in any of the data sets analyzed here. Moreover, the signal power of most of the time

**Table 1.** Linear Trends of Deseasonalized Surface Ocean Variables at Stations ALOHA and Kahe

Variable (Units)	<i>n</i> <sup>a</sup>	ALOHA			Kahe		
		Conf. <sup>b</sup>	Trend <sup>c</sup> (year <sup>-1</sup> )	SE <sup>d</sup> (year <sup>-1</sup> )	Conf.	Trend (year <sup>-1</sup> )	SE (year <sup>-1</sup> )
Temperature (°C)	240	nd <sup>e</sup>			nd		
Salinity	240	>90%	0.0116	0.0014	>90%	0.0138	0.0015
<i>p</i> CO <sub>2</sub> (μatm)	217	>95%	1.78	0.08	>95%	1.79	0.10
	240	>95%	1.81	0.07			
[H <sup>+</sup> ] (nmol kg <sup>-1</sup> )	217	>95%	0.031	0.002	>95%	0.031	0.002
	240	>95%	0.032	0.001			
Ω <sub>arag</sub>	217	>90%	-0.0086	0.0006	>90%	-0.0086	0.0008
	240	>95%	-0.0086	0.0006			
<i>n</i> DIC (μmol kg <sup>-1</sup> )	217	>99%	1.15	0.05	>95%	1.11	0.05
	240	>99%	1.12	0.04			
<i>n</i> TA (μeq kg <sup>-1</sup> )	217	>99%	0.20	0.04	>90%	0.13	0.06
	240	>99%	0.15	0.03			
Chl <i>a</i> (mg m <sup>-3</sup> )	230	nd			nd		
	240	nd					
MLD (m)	240	nd			nd		
<i>p</i> CO <sub>2atm</sub> (μatm) <sup>f</sup>	240	>99%	1.77	0.01			

<sup>a</sup>*n* = length of data vector over period of observation: 217 points (March 1991 to October 2012), 230 points (November 1989 to October 2012), or 240 points (November 1988 to October 2012).

<sup>b</sup>Conf. = confidence level with which secular trend is detected by MTM analysis.

<sup>c</sup>Trend = slope of linear regression of data vector following subtraction of significant (>95% confidence) annual and higher-frequency narrowband signals.

<sup>d</sup>SE = standard error of regression slope.

<sup>e</sup>nd = secular trend not detected above red noise background at 90% confidence level.

<sup>f</sup>Atmospheric CO<sub>2</sub> mole fractions from Mauna Loa Observatory (MLO) converted to partial pressures at ALOHA sea surface conditions (see section 2).

**Table 2.** Mean Values, Residuals, and Residual Comparisons Between Sites

Variable (Units)	<i>n</i> <sup>a</sup>	ALOHA			Kahe			Kahe Versus ALOHA	
		Mean <sup>b</sup>	SE <sup>c</sup>	RMS Resid <sup>d</sup>	Mean	SE	RMS Resid	<i>r</i> <sup>2e</sup>	RMS ΔResid <sup>f</sup>
Temperature (°C)	240	24.82	0.04	0.582	25.81	0.04	0.546	0.722	0.311
Salinity	240	35.08	0.01	0.150	34.90	0.01	0.155	0.420	0.166
<i>p</i> CO <sub>2</sub> (μatm)	217	350.1	0.9	7.1	353.4	1.0	8.9	0.259	8.1
	240	347.9	0.9	7.1					
[H <sup>+</sup> ] (nmol kg <sup>-1</sup> )	217	8.12	0.02	0.14	8.22	0.02	0.18	0.253	0.16
	240	8.08	0.02	0.14					
Ω <sub>arag</sub>	217	3.67	0.01	0.06	3.73	0.01	0.07	0.168	0.07
	240	3.68	0.01	0.06					
<i>n</i> DIC (μmol kg <sup>-1</sup> )	217	1976.3	0.6	4.7	1972.0	0.6	4.6	0.337	4.3
	240	1975.1	0.6	4.7					
<i>n</i> TA (μeq kg <sup>-1</sup> )	217	2303.6	0.3	3.7	2304.6	0.3	5.1	0.154	5.0
	240	2303.6	0.2	3.7					
Chl <i>a</i> (mg m <sup>-3</sup> )	230	0.087	0.002	0.023	0.076	0.001	0.017	0.176	0.022
	240	0.089	0.002	0.024					
MLD (m)	240	59.9	1.1	16.2	43.0	1.1	16.5	0.074	19.4
<i>p</i> CO <sub>2atm</sub> (μatm) <sup>g</sup>	240	363.0	0.8	1.5					

<sup>a</sup>*n* = length of data vector over period of observation: 217 points (March 1991 to October 2012), 230 points (November 1989 to October 2012), or 240 points (November 1988 to October 2012).

<sup>b</sup>Mean of data vector following subtraction of significant (>95% confidence) annual and higher-frequency narrowband signals.

<sup>c</sup>SE = standard error of the mean.

<sup>d</sup>Root-mean-square of residuals remaining after further subtraction of mean or linear trend, if a trend was detected (>90% confidence).

<sup>e</sup>Correlation coefficient between ALOHA and Kahe residuals with no time lag.

<sup>f</sup>Root-mean-square of the differences between ALOHA and Kahe residuals.

<sup>g</sup>Atmospheric CO<sub>2</sub> mole fractions from MLO converted to partial pressures at ALOHA sea surface conditions (see section 2).

**Table 3.** Percent of Variance Characterized as Periodic Signals, Linear Trend, or Residuals

Variable	$n^a$	ALOHA			Kahe		
		Narrow Band <sup>b</sup>	Linear Trend	Resid <sup>c</sup>	Narrow Band	Linear Trend	Resid
Temperature	240	72.0	nd <sup>d</sup>	28.0	71.6	nd	28.4
Salinity	240	11.8	19.7	68.5	13.2	23.6	63.2
$p\text{CO}_2$	217	33.9	47.0	19.1	32.0	41.6	26.4
	240	28.9	53.8	17.3			
$[\text{H}^+]$	217	40.5	39.5	20.0	37.8	33.9	28.3
	240	34.7	46.4	18.9			
$\Omega_{\text{arag}}$	217	32.6	30.5	36.9	27.3	25.3	47.4
	240	28.0	36.2	35.8			
$n\text{DIC}$	217	17.7	57.9	24.4	20.1	55.5	24.4
	240	15.2	62.0	22.8			
$n\text{TA}$	217	13.4	8.5	78.1	8.3	2.4	89.3
	240	13.3	6.7	80.0			
Chl $a$	230	40.2	nd	59.8	35.9	nd	64.1
	240	37.8	nd	62.2			
MLD	240	43.8	nd	56.2	38.7	nd	61.3
$p\text{CO}_{2\text{atm}}^e$	240	3.5	95.1	1.4			

<sup>a</sup> $n$  = length of data vector over period of observation: 217  $n$  points (March 1991 to October 2012), 230 points (November 1989 to October 2012), or 240 points (November 1988 to October 2012).

<sup>b</sup>Includes significant (>95% confidence) annual and higher-frequency narrowband signals.

<sup>c</sup>Resid = residual variance.

<sup>d</sup>nd = secular trend not detected above red noise background at 90% confidence level.

<sup>e</sup>Atmospheric  $\text{CO}_2$  mole fractions from MLO converted to partial pressures at ALOHA sea surface conditions (see section 2).

series in this frequency range was distinctly low (Figure 2). It is possible that ENSO effects at these sites, if they exist, are phased too randomly to be detected as quasiperiodic signals using MTM analysis over these relatively short time series. Decadal and lower frequency signals cannot be resolved from these time series, and in this analysis, they remain part of the residuals after deseasonalization and linear detrending of the data vectors (Tables 2 and 3 and Figure S2).

The observation of significant (>95% confidence) increasing secular trends in  $p\text{CO}_2$ ,  $[\text{H}^+]$ , and  $n\text{DIC}$  at both sites (Table 1) is consistent with the equilibration of the surface ocean with the increasing atmospheric  $\text{CO}_2$  pool [Dore et al., 2009; Keeling et al., 2004]. Although physical and biological modulations of the surface ocean  $\text{CO}_2$  system in the NPSG on seasonal and interannual timescales have been observed [Dore et al., 2003; Brix et al., 2004; Keeling et al., 2004; Dore et al., 2009], the nearly identical rate of increase of  $p\text{CO}_2$  at both sites with that of  $p\text{CO}_{2\text{atm}}$  (Table 1) suggests that the secular  $p\text{CO}_2$  trend can be explained by the atmospheric driver alone. No temperature trends of the surface ocean at these sites could be detected above the noise of the 24 year time series (Table 1). Similarly, we detected no significant change to surface chl  $a$  concentrations in our data sets, though both positive and negative chl  $a$  trends have previously been suggested to exist in the region [Boyce et al., 2014, and references therein].

Despite their many apparent similarities (Figure 1), these sites display significant differences in mean values of surface ocean biogeochemical variables (Table 2). Warmer temperatures at Kahe likely result from its leeward location, where lower winds result in reduced mixing with cooler subsurface waters and in less evaporative cooling. Reduced cloud cover in the immediate lee of the islands [Xie et al., 2001] may also contribute to greater insolation at Kahe than at ALOHA, as does, to a minor extent, the small difference in latitude between the stations. However, there may also be some temperature bias introduced because Kahe is usually sampled near midday while ALOHA is sampled around the clock. Slightly higher  $p\text{CO}_2$  and  $[\text{H}^+]$  and slightly lower  $\Omega_{\text{arag}}$  at Kahe reflect both the small excess of  $n\text{DIC}$  observed there and the temperature difference between the sites (Table 2). Higher chl  $a$  at ALOHA is likely due to phytoplankton photoadaptation within a deeper mixed layer [Winn et al., 1995]; similar windward-leeward differences in chl  $a$  across the Hawaiian Ridge have been reported at 24°N [Venrick, 1991].

The characterization of variance differs substantially among the variables examined (Table 3). Annual (plus higher frequency) signals are particularly important sources of variance for temperature, MLD, chl  $a$ , and



the temperature-dependent CO<sub>2</sub> system variables ( $p\text{CO}_2$ ,  $[\text{H}^+]$ , and  $\Omega_{\text{arag}}$ ). For the CO<sub>2</sub> system variables other than  $n\text{TA}$ , the linear trend is an important, and in some cases the dominant identifiable source of variance. Unidentified sources of variance dominate the time series of salinity, MLD, chl  $a$ , and  $n\text{TA}$ . For salinity, interannual variability appears to be important [Dore *et al.*, 2003; Lukas and Santiago-Mandujano, 2008], but these signals are either aperiodic or insufficiently sampled to rise above the red noise background (Figures 1 and S2). For MLD and chl  $a$ , it is likely that significant sources of variability exist at very high frequencies that are not resolved at the 10 year<sup>-1</sup> station occupation frequency, such as those expected from weather fluctuations, storm-induced mixing and nutrient entrainment events, or episodic phytoplankton blooms [Dore *et al.*, 2008]. The relative constancy of  $n\text{TA}$  makes it difficult to identify specific modes of its variability; however, the RMS of residuals for  $n\text{TA}$  is only ~0.2% of the overall mean value (Table 2), which is approximately the same magnitude as the analytical error of the  $n\text{TA}$  measurement. A period of slightly elevated (~0.3% of mean)  $n\text{TA}$  at Kahe in 2000–2001 that contributes to residual variance and noticeably affects the calculated CO<sub>2</sub> system variables (Figures 1 and S2) is not easily explained and may result from sample collection or storage artifacts.

All observed CO<sub>2</sub> system trends are common to both ALOHA and Kahe (Table 1), suggesting common drivers across the region (e.g., net transport of anthropogenic CO<sub>2</sub> from the atmosphere into the surface ocean). This close agreement (e.g., linear trends within <4% for  $n\text{DIC}$  and <1% for  $p\text{CO}_2$  and  $[\text{H}^+]$ ) provides a strong corroboration of our earlier documentation of the progressive acidification of surface ocean waters at ALOHA [Dore *et al.*, 2009; Bates *et al.*, 2014]. Moreover, the consistency of trends at these physically contrasting sites supports the regional representativeness of ALOHA and suggests the likely viability of extrapolating temporal trends observed in the extensive surface data sets from ALOHA to the regional spatial scale.

#### Acknowledgments

We thank all past and present HOT personnel for data collection. R. Lukas and two anonymous reviewers kindly provided helpful comments on earlier versions of this paper. HOT data are publicly available at <http://hahana.soest.hawaii.edu/hot/>. This work was principally supported by the National Science Foundation (most recently through grant OCE-1260164), with additional contributions from the National Oceanic and Atmospheric Administration, the Department of Energy, the State of Hawaii, and the Gordon and Betty Moore Foundation.

The Editor thanks two anonymous reviewers for their assistance in evaluating this paper.

#### References

- Bates, N. R., Y. M. Astor, M. J. Church, K. Currie, J. E. Dore, M. González-Dávila, L. Lorenzoni, F. Muller-Karger, J. Olafsson, and J. M. Santana-Casiano (2014), A time-series view of changing surface ocean chemistry due to ocean uptake of anthropogenic CO<sub>2</sub> and ocean acidification, *Oceanography*, 27(1), 94–109.
- Boyce, D. G., M. Dowd, M. R. Lewis, and B. Worm (2014), Estimating global chlorophyll changes over the past century, *Prog. Oceanogr.*, 122, 163–173.
- Brix, H., N. Gruber, and C. D. Keeling (2004), Interannual variability of the upper ocean carbon cycle at station ALOHA near Hawaii, *Global Biogeochem. Cycles*, 18, GB4019, doi:10.1029/2004GB002245.
- Chavanne, C., P. Flament, and K.-W. Gurgel (2010), Interactions between a submesoscale anticyclonic vortex and a front, *J. Phys. Oceanogr.*, 40(8), 1802–1818.
- Chen, F., W.-J. Cai, Y. Wang, Y. M. Rii, R. R. Bidigare, and C. R. Benitez-Nelson (2008), The carbon dioxide system and net community production within a cyclonic eddy in the lee of Hawaii, *Deep Sea Res., Part II*, 55(10), 1412–1425.
- Church, M. J., M. W. Lomas, and F. Muller-Karger (2013), Sea change: Charting the course for biogeochemical ocean time-series research in a new millennium, *Deep Sea Res., Part II*, 93, 2–15.
- Clayton, T. D., and R. H. Byrne (1993), Spectrophotometric seawater pH measurements: Total hydrogen ion concentration scale calibration of *m*-cresol purple and at-sea results, *Deep Sea Res., Part I*, 40(10), 2115–2129.
- Deser, C., M. A. Alexander, and M. S. Timlin (2003), Understanding the persistence of sea surface temperature anomalies in midlatitudes, *J. Clim.*, 16(1), 57–72.
- Dickson, A. G., C. L. Sabine, and J. R. Christian (2007), Guide to best practices for Ocean CO<sub>2</sub> measurements, *Spec. Publ. 3*, PICES, Sidney, B. C., Canada. [Available at [http://cdiac.ornl.gov/oceans/Handbook\\_2007.html](http://cdiac.ornl.gov/oceans/Handbook_2007.html).]
- Doney, S. C., V. J. Fabry, R. A. Feely, and J. A. Kleypas (2009), Ocean acidification: The other CO<sub>2</sub> problem, *Annu. Rev. Mar. Sci.*, 1, 169–192.
- Dore, J. E., R. Lukas, D. W. Sadler, and D. M. Karl (2003), Climate-driven changes to the atmospheric CO<sub>2</sub> sink in the subtropical North Pacific Ocean, *Nature*, 424(6950), 754–757.
- Dore, J. E., R. M. Letelier, M. J. Church, R. Lukas, and D. M. Karl (2008), Summer phytoplankton blooms in the oligotrophic North Pacific Subtropical Gyre: Historical perspective and recent observations, *Prog. Oceanogr.*, 76(1), 2–38.
- Dore, J. E., R. Lukas, D. W. Sadler, M. J. Church, and D. M. Karl (2009), Physical and biogeochemical modulation of ocean acidification in the central North Pacific, *Proc. Natl. Acad. Sci. U.S.A.*, 106(30), 12,235–12,240.
- Doty, M. S., and M. Oguri (1956), The island mass effect, *J. Cons. Perm. Int. Explor. Mer.*, 22(1), 33–37.
- Ghil, M., et al. (2002), Advanced spectral methods for climatic time series, *Rev. Geophys.*, 40(1), 1003, doi:10.1029/2000RG000092.
- Gilmartin, M., and N. Revelante (1974), The 'island mass' effect on the phytoplankton and primary production of the Hawaiian Islands, *J. Exp. Mar. Biol. Ecol.*, 16(2), 181–204.
- Gruber, N., C. D. Keeling, and N. R. Bates (2002), Interannual variability in the North Atlantic Ocean carbon sink, *Science*, 298(5602), 2374–2378.
- Hassett, R. P., and G. W. Boehlert (1999), Spatial and temporal distributions of copepods to leeward and windward of Oahu, Hawaiian Archipelago, *Mar. Biol.*, 134(3), 571–584.
- Karl, D. M., and R. Lukas (1996), The Hawaii Ocean Time-series (HOT) program: Background, rationale and field implementation, *Deep Sea Res., Part II*, 43(2-3), 129–156.
- Karl, D. M., R. Letelier, D. Hebel, L. Tupas, J. Dore, J. Christian, and C. Winn (1995), Ecosystem changes in the North Pacific subtropical gyre attributed to the 1991–92 El Niño, *Nature*, 373(6511), 230–234.

- Keeling, C. D., H. Brix, and N. Gruber (2004), Seasonal and long-term dynamics of the upper ocean carbon cycle at Station ALOHA near Hawaii, *Global Biogeochem. Cycles*, *18*, GB4006, doi:10.1029/2004GB002227.
- Keeling, R. F., S. C. Piper, A. F. Bollenbacher, and J. S. Walker (2009), Atmospheric CO<sub>2</sub> records from sites in the SIO air sampling network, in *Trends: A Compendium of Data on Global Change*, Carbon Dioxide Information Analysis Center, Oak Ridge National Laboratory, U.S. Department of Energy, Oak Ridge, Tenn., doi:10.3334/CDIAC/atg.035. [Available at <http://cdiac.ornl.gov/trends/co2/sio-mlo.html>.]
- Kroeker, K. J., R. L. Kordas, R. Crim, I. E. Hendriks, L. Ramajo, G. S. Singh, C. M. Duarte, and J.-P. Gattuso (2013), Impacts of ocean acidification on marine organisms: Quantifying sensitivities and interaction with warming, *Global Change Biology*, *19*(6), 1884–1896.
- Letelier, R. M., J. E. Dore, C. D. Winn, and D. M. Karl (1996), Seasonal and interannual variations in photosynthetic carbon assimilation at Station ALOHA, *Deep Sea Res., Part II*, *43*(2), 467–490.
- Letelier, R. M., D. M. Karl, M. R. Abbott, P. Flament, M. Freilich, R. Lukas, and T. Strub (2000), Role of late winter mesoscale events in the biogeochemical variability of the upper water column of the North Pacific Subtropical Gyre, *J. Geophys. Res.*, *105*(C12), 28,723–28,739.
- Lukas, R., and F. Santiago-Mandujano (1996), Interannual variability of Pacific deep- and bottom-waters observed in the Hawaii Ocean Time-series, *Deep Sea Res., Part II*, *43*(2–3), 243–255.
- Lukas, R., and F. Santiago-Mandujano (2008), Interannual to interdecadal salinity variations observed near Hawaii: Local and remote forcing by surface freshwater fluxes, *Oceanography*, *21*(1), 46–55.
- Lumpkin, R., and P. J. Flament (2013), Extent and energetics of the Hawaiian Lee Countercurrent, *Oceanography*, *26*(1), 58–65.
- Mann, M. E., and J. M. Lees (1996), Robust estimation of background noise and signal detection in climatic time series, *Clim. Change*, *33*(3), 409–445.
- Phillips, H. E., and T. M. Joyce (2007), Bermuda's tale of two time series: Hydrostation S and BATS, *J. Phys. Oceanogr.*, *37*(3), 554–571.
- Pierrot, D., E. Lewis, and D. W. R. Wallace (2006), MS Excel program developed for CO<sub>2</sub> system calculations, *Publ. ORNL/CDIAC-105a*, Carbon Dioxide Information Analysis Center, Oak Ridge National Laboratory, U.S. Department of Energy, Oak Ridge, Tenn., doi:10.3334/CDIAC/otg.CO2SYS\_XLS\_CDIAC105a.
- Provoost, P., S. van Heuven, K. Soetaert, R. W. P. M. Laane, and J. J. Middelburg (2010), Seasonal and long-term changes in pH in the Dutch coastal zone, *Biogeosciences*, *7*(11), 3869–3878.
- Qiu, B., D. A. Koh, C. Lumpkin, and P. Flament (1997), Existence and formation mechanism of the North Hawaiian Ridge Current, *J. Phys. Oceanogr.*, *27*(3), 431–444.
- Roden, G. I. (1991), Effects of the Hawaiian Ridge upon oceanic flow and thermohaline structure, *Deep-Sea Res.*, *38*(S1), S623–S654.
- Sakamoto, C. M., D. M. Karl, H. W. Jannasch, R. R. Bidigare, R. M. Letelier, P. M. Walz, J. P. Ryan, P. S. Polito, and K. S. Johnson (2004), Influence of Rossby waves on nutrient dynamics and the plankton community structure in the North Pacific subtropical gyre, *J. Geophys. Res.*, *109*, C05032, doi:10.1029/2003JC001976.
- Thomson, D. J. (1982), Spectrum estimation and harmonic analysis, *Proc. IEEE*, *70*(9), 1055–1096.
- Thoning, K. W., D. R. Kitzis, and A. Croswell (2014), Atmospheric carbon dioxide dry air mole fractions from quasi-continuous measurements at Barrow, Alaska; Mauna Loa, Hawaii; American Samoa; and South Pole, 1973–2013, Version: 2014-06-27. [Available at [ftp://aftp.cmdl.noaa.gov/data/trace\\_gases/co2/in-situ/surface/](ftp://aftp.cmdl.noaa.gov/data/trace_gases/co2/in-situ/surface/).]
- Venrick, E. L. (1991), Mid-ocean ridges and their influence on the large-scale patterns of chlorophyll and production in the North Pacific, *Deep-Sea Res.*, *38*(S1), S83–S102.
- Winn, C. D., L. Campbell, J. R. Christian, R. M. Letelier, D. V. Hebel, J. E. Dore, L. Fujieki, and D. M. Karl (1995), Seasonal variability in the phytoplankton community of the North Pacific Subtropical Gyre, *Global Biogeochem. Cycles*, *9*(4), 605–620, doi:10.1029/95GB02149.
- Wootton, J. T., and C. A. Pfister (2012), Carbon system measurements and potential climatic drivers at a site of rapidly declining ocean pH, *PLoS One*, *7*(12), e53396, doi:10.1371/journal.pone.0053396.
- Xie, S.-P., W. T. Liu, Q. Liu, and M. Nonaka (2001), Far-reaching effects of the Hawaiian Islands on the Pacific Ocean-atmosphere system, *Science*, *292*(5524), 2057–2060.